A Novel RoF System Integrating Optical Fiber and FSO Channel with Polarization Multiplexing PAM4 Downlink Signals

Yufeng Shao (syufeng@163.com)
Chongqing Three Gorges University
Qing Tian
Chongqing Three Gorges University
Anrong Wang
Chongqing Three Gorges University
Ni Yu
Chongqing Three Gorges University
Qiming Yang
Chongqing Three Gorges University
Linfang Yi
Chongqing Three Gorges University
Jie Yuan
Chongqing Three Gorges University
Yanlin Li
Chongqing Three Gorges University
Peng Chen
Chongqing Three Gorges University
Chong Li
Chongqing Three Gorges University
Shuanfan Liu
Chongqing Three Gorges University
Renjie Zuo
Chongqing Three Gorges University

Research Article

Keywords: Free-space optical communication, Fiber optics communications, PAM4, Eye diagram, BER

Posted Date: December 2nd, 2022

DOI: https://doi.org/10.21203/rs.3.rs-2318998/v1

Abstract

A novel radio over fiber (RoF) system with polarization multiplexing 4-ary pulse amplitude modulation (PAM4) downlink signals is proposed and designed. The generated downstream signal is transmitted over 25km smf-28 and 100m optical wireless channel. The 60GHz millimeter-wave is generated by the beating of two continuous light waves, and the high frequency signal is demodulated by using self-mixing detection method. We analyzed the transceiver and transmission performance of the introduced polarization multiplexing RoF-FSO system. The results demonstrate this scheme can effectively improve the spectral efficiency of downlink broadband access signals, and be applied in the future broadband access network.

1. Introduction

With the emergence of the information age and the rapid development of communication technology, there is an increasing demand for high-speed, large bandwidth, and flexible wireless access. Higher bandwidth is considered to be solutions with the next generation high-speed wireless communication technology [1]. As we know, free space optical (FSO) communication has become a competitive technology to provide high-speed and large bandwidth wireless access [2]. FSO technology has the advantages of high speed, large bandwidth, strong security, and easy installation [3]. Especially, FSO communication links can replace conventional fiber-optic links in complex terrain environments [4]. Its convenience brings users more secure and flexible information transmission application experience [5]. However, due to the atmospheric turbulence on optical wireless signals transmission in free space, the communication signals instability and the signals distortion often occurs [6]. Furthermore, since the FSO system only supports broadband communication access to outdoor terminals the radio over fiber (RoF) system can seamlessly connect to indoor wireless access terminal for multiple types of users, so we consider integrating RoF system access after the FSO receiver [7]. RoF system combines the merits with large capacity and high bandwidth in optical communication and high stability and anti-interference on microwave communication technology [8]. Hence, this system has become a promising alternative scheme in broadband wireless access systems in the future, and has attracted extensive attention from the academic community [9, 10]. The polarization multiplexing system has simple structure, which can double the transmission capacity and increase the frequency spectrum utilization [11, 12]. To further improve the transmission capacity of broadband access systems, the polarization multiplexing technology combined with the 4-ary pulse amplitude modulation (PAM4) technology is also be introduced to achieve higher frequency band utilization and higher transmission rate [13].

In this paper, a novel radio over fiber free space optics (RoF-FSO) communication system with 10Gbit/s polarization multiplexing PAM4 downlink signals is introduced and discussed. The optical spectra diagrams, RF spectrums, Q factors, eye-diagrams and bit error rate (BER) of 10Gbit/s PAM4 downstream signals in polarization multiplexing RoF-FSO system are analyzed. The results show that this broadband communication scheme can effectively integrate RoF access with FSO transmission system and achieve high spectral efficiency application in future high-speed access network.

2. System Setup

Figure 1 shows the system configuration of the proposed scheme. At the transmitter, two continuous waves (CWs) with 193.1THz and 193.16THz worked frequencies are generated by two external cavity lasers (ECLs), and the frequency tone spacing is 60 GHz. The CW_1 light is divided into equal two parallel optical carriers through the polarization beam $splitter_1$. Each one is modulated by a single-arm Mach-Zehnder modulator (MZM) using 10Gbit/s PAM4 electrical signal, then two parallel optical carriers recombine through the polarization beam combiner to form a polarized light. Through one symmetrical 3dB optical coupler, the modulated optical carrier is coupled with CW_2 (193.16THz) and transmitted on the 25km single-mode fiber. The used optical fiber parameters are shown in Table I. Then the signal is input to FSO system which consisting of a transmitting telescope, the free space link and a receiving telescope. The free-space link distance is 100m, and the optical signal attenuation value under sunny condition is 10dB/km. The transmitter aperture is 5cm, and the receiver aperture is 20cm. The beam divergence is 2mard, as shown in Table II. Since the optical signal power will attenuate in optical fiber and free space transmission, one erbium-doped optical fiber amplifier (EDFA) is used. At the receiver, signal after transmission is split two optical paths by polarization beam $splitter_2$ for demodulation.

Table I. Optical fiber parameters

Parameters	**Values**
Length (km)	25
Attenuation (dB/km)	0.2
Dispersion (ps/nm/km)	16.75
Dispersion slop (ps/nm^2/km)	0.075
Core area (μm^2)	80

Table II. FSO link parameters

Parameters	Values
Length (m)	100
The transmitter aperture diameter (cm)	5
The receiver aperture diameter (cm)	20
Attenuation (dB/km)	10
The beam divergence (mard)	2

In each received signal path, the 60GHz millimeter wave is generated in the photodetector (PIN-PD) by two light waves beating together in the photoelectric conversion process. Two standards horn antennas are used to transmit-receive the 60GHz millimeter wave signal. The received signal is demodulated by using the self-mixing detection technology. Using adjustable phase shifter to compensate phase deflection, which is conducive to reducing the influence of phase noise. Because no local oscillator is used, the system cost budget is further reduced. After self-mixing process, the high-frequency signal is filtered out by two low-pass filters (LPFs), and in which the cut-off frequency value is 0.75GHz. Then, the 3R regenetors are used to recover the original data information.

3. Results

Figure 2 (a) and (b) respectively show the time domain waveforms of PAM4 $signal_1$ and $signal_2$ before transmission. After transmission and polarization demultiplexing, the time-domain waveforms of PAM4 $signal_1$ and $signal_2$ are shown in Fig. 2 (c) and (d) respectively. Due to the chirp effect and the insertion loss of both transmitting and receiving telescopes in the FSO link, the received optical power will become lower. The time domain waveforms all show slight amplitude changes, but no error if choose the right decision position.

Figure 3 (a) shows the optical spectrums before transmission, after optical fiber transmission is shown in Fig. 3 (b), and after FSO link transmission is shown in Fig. 3 (c). There is no wavelength shift phenomenon, which proves that the frequency stability is good. The signal attenuation will occur in the optical fiber and FSO links have influence. After transmission, the received optical power is lower than fiber input power.

The demodulated electrical spectrums of PAM4 $signal_1$ and $signal_2$ before transmission are shown in Fig. 4 (a) and (b). After transmission and polarization demultiplexing, the electrical spectrums of PAM4 $signal_1$ and $signal_2$ though self-mixing detection and two LPFs filtering are shown in Fig. 4 (c) and (d). As the bit transmission rate is 10Gbit/s, the main lobe bandwidth of the electrical spectrum is 5GHz. The energy of main lobe and side lobe attenuates in different degrees, and the side lobe attenuation is more serious than the main lobe. However, since the frequency band energy is mainly concentrated in the main lobe, this attenuation has little effect on the signal.

Q factors v/s bit period of PAM4 $signal_1$ and PAM4 $signal_2$ after transmission over 25km SMF and 100m FSO downstream at a BER of 10^{-3}, as shown in Fig. 5 (a) and (b). Two eye diagrams of PAM4 $signal_1$ and PAM4 $signal_2$ after transmission over 25km SMF and 100m FSO downlink are shown in Fig. 5 (c) and (d). For PAM4 $signal_1$, the demodulated signal optimal decision point is 0.5bit time. For PAM4 $signal_2$, the optimal decision point for demodulated signal is 0.46bit time. Although the eyelid becomes thicker, the eye diagrams are still clear.

Figure 6 shows the received power versus BER of two downstream PAM4 signals. The received power values of two PAM4 signals in the back-to-back case are − 22.35dBm and − 22.55dBm respectively (at a BER of 10^{-3}), which is significantly better than that after downlink transmission. At the end of 25km SMF-28 and 100m FSO channel, the received power values are − 21.19dBm and − 21.10dBm respectively, and the BER performance of the two received downstream signals after depolarization multiplexing is similar. After transmission and depolarization multiplexing, the receiver sensitivities of PAM4 $signal_1$ and PAM4 $signal_2$ are 1.16dB and 1.45 dB (at a BER of 10^{-3}).

4. Conclusion

In this paper, we proposed and demonstrated a polarization multiplexing RoF-FSO communication system, which can transmit PAM4 signals over 25km optical fiber and 100m FSO links. The characteristics of PAM4 downstream signals are tested, such as time domain waveforms, optical spectra diagrams, electrical spectrums, Q factors v/s bit period diagrams, eye-diagrams and curves of received power versus BER after transmission. This scheme integrates high-speed optical fiber transmission and FSO communication systems, and can effectively improve the spectral efficiency of downlink broadband access signals. Since it is especially suitable for the final access areas where the optical fiber is difficult to be laid in and only FSO systems can be used, it is expected to be applied in the future broadband access network.

Declarations

Acknowledgments

This work is partially supported by the National Natural Science Foundation of China (61107064); Science and Technology Research Program of Chongqing Municipal Education Commission (KJZD-M201901201); Chongqing University Innovation Team Founding (KJTD201320); Chongqing Science and Technology Commission Foundation (cstc2018jcyjAX0038, cstc2016jcyjA0246); Chongqing Key Laboratory of Geological Environment Monitoring and Disaster Early-warning in Three Gorges Reservoir Area(ZD2020A0102, ZD2020A0103); Youth Project of Science and Technology Research Program of Chongqing Education Commission of China (KJQN201801227); Chongqing Three Gorges Reservoir Area Geological Environment Monitoring and Disaster Warning Key Laboratory Open Fund Major Project (ZD2020A0104); Science and Technology Research Program of Chongqing Education Commission of

China (KJ1401005); Chongqing Three Gorges College Excellent Achievement Transformation Project (18CGZH03). Postgraduate scientific research innovation project of Chongqing Three Gorges University (YJSKY21015, YJSKY22011, YJSKY22014, YJSKY22016, YJSKY22017, YJSKY22021).

References

1. Shao, Y. F., Chen, F. P., Chen, L., Shen, S. L., Wang, A. R., Luo, Y. X., & Tan, Z. F. (2016). DP-DQPSK optical access system integrated with fiber and free-space downlink for high spectral efficiency application[J]. *Optics and Photonics Journal*, *6*(08), 108. https://doi.org/10.4236/opj.2016.68B018.
2. Liang, L. L., Wei, D., & Li, M. (2017). Wireless physical layer security based on channel pre-compensation for PolSK modulated systems. *2017 IEEE 9th International Conference on Communication Software and Networks*, 357–361. https://doi.org/10.1109/ICCSN.2017.8230135
3. Long, Y., Shao, Y. F., Wang, A. R., Hu, Q. Z., Lei, G. P., Liu, Y., Hu, Z. Q., Wang, Z., & Yang, J. (2020). Research on DP-DB FSO access system for three gorges reservoir area with special landform[J]. *Journal of Optoelectronics Laser*, *31*, 773–778. https://doi.org/10.16136/j.joel.2020.07.0007.
4. Baiwa, R., & Verma, P. (2018). Performance analysis of FSO system for advanced modulation formats under different weather conditions, *2018 Second International Conference on Intelligent Computing and Control Systems (ICICCS)*. 1490–1495. https://doi.org/10.1109/ICCONS.2018.8663090
5. Shao, Y. F., Chen, L., Wang, A. R., Zhao, Y. J., Long, Y., & Ji, X. P. (2018). Analysis of different sub-carrier allocation of M-ary QAM-OFDM downlink in RoF system[J]. *Optoelectronics Letters*, *14*, 40–43. https://doi.org/10.1007/s11801-018-7142-x.
6. Chen, F. P., Shao, Y. F., Chen, L., Shen, S. L., Wang, A. R., Luo, Y. X., & Zhao, Y. J. (2017). Study on RZ-4PAM downstream signals with duty cycles of 33% and 50% for optical access system application. *Optoelectronics Letters*, *13*, 163–166. https://doi.org/10.1007/s11801-017-6197-4.
7. Chen, S. H., Yan, X. Q., Chen, Li, S., & Yang, L. (2021). Performance analysis of hybrid dual-hop PLC-FSO communication system[J]. *Journal on Communications*, *42*(10), 243–250. doi: 10.11959/j.issn.1000-436x.2021199.
8. Xu, Z. X., Xu, G. J., & Zheng, Z. Q. (2021). BER and Channel Capacity Performance of an FSO Communication System over Atmospheric Turbulence with Different Types of Noise[J]. *Sensors (Basel, Switzerland)*, *21*(10), 3454–3454. https://doi.org/10.3390/s21103454.
9. Todorović, J., Jakšić, B., Spalević, P., Banđur, Đ., & Banđur, M. (2020). Analysis of signal quality in FSO systems with Polsk modulation[J]. *Serbian Journal of Electrical Engineering*, *17*(2), 171–186. https://doi.org/10.2298/SJEE2002171T.
10. Wang, Z. Y., Xiao, Y. Q., Wang, S. T., Yan, Y. S. Y., Wang, B. S., Chen, Y. T., Zhou, Z. H., He, J., & Yang, L. (2021). Probabilistic shaping-based constellation encryption for physical layer security in OFDM RoF system[J]. *Optics Express*, *29*, 17890–17901. https://doi.org/10.1364/OE.424661.

11. Tian, Q., Shao, Y. F., Wang, A. R., Wang, Z., Yang, J., Yu, N., Yang, Q. M., Yi, L. F., Yuan, J., Li, Y. L., Chen, P., Li, C., Liu, S. F., & Zuo, R. J. (2022). A RoF-FSO Communication System Using 10Gbit/s Polsk PAM4 Downstream Signals[C]//*ITM Web of Conferences*. EDP Sciences, **45**. https://doi.org/10.1051/itmconf/20224502004
12. Kovachev, Y., & Mitsev, T. (2013). Trends in increasing the channel capacity of FSO systems[C]. *Annual ICEST Conference*. 26–28.
13. Zhang, L., Xiang, P., Zhao, J., Zhou, H., Zheng, J. L., Zhang, H., Shen, Y. H., & Pu, T. (2019). Performance evaluation for polarization shift keying modulation in atmospheric turbulence channel[C], *2019 18th International Conference on Optical Communications and Networks (ICOCN)*. 1–3. https://doi.org/10.1109/ICOCN.2019.8934063

Figures

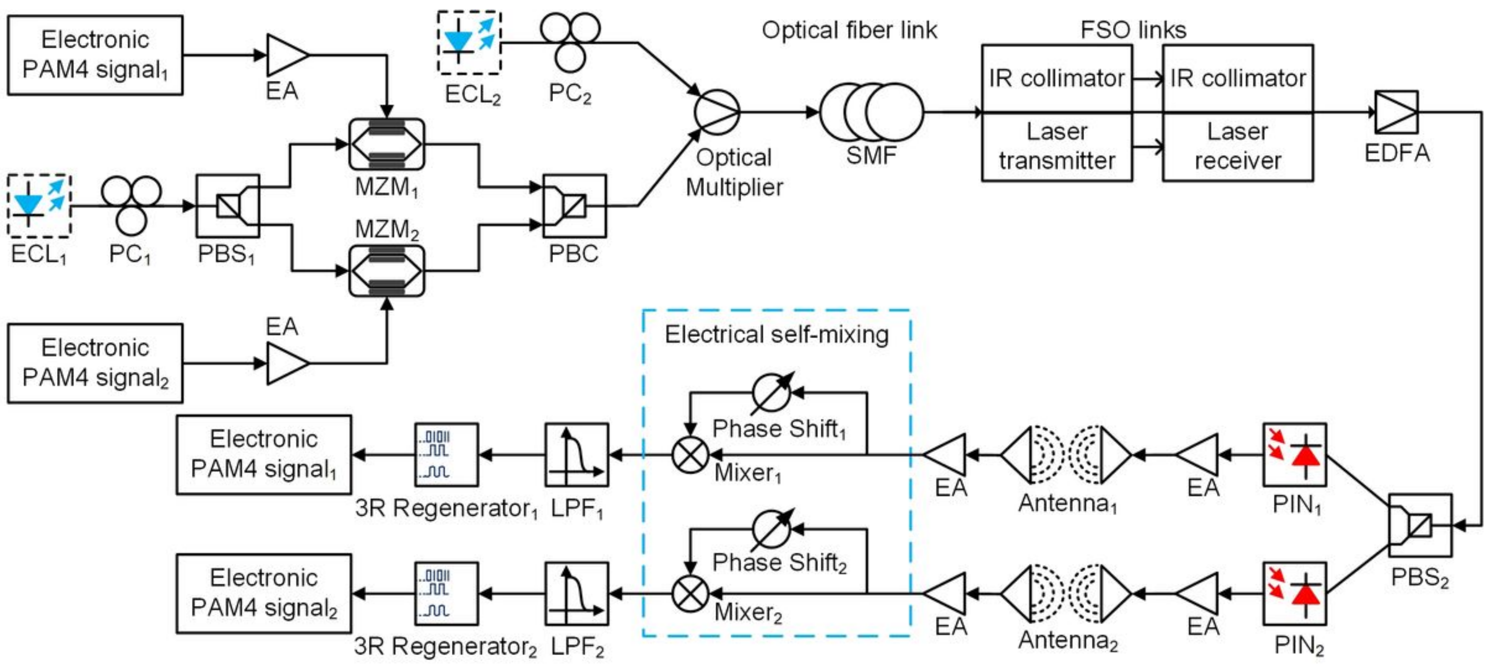

Figure 1

System configuration. (ECL external cavity laser;PC: polarization controller; PBS: polarization beam splitter; PBC: polarization beam combiner ; MZM: Mach-Zehnder modulator; SMF: single mode fiber; OBF: optical band pass filter; FSO: free space optical communication; EDFA erbium-doped optical fiber amplifier; PIN: positive intrinsic-negative ; EA: electric amplifier ; LPF: low pass filter)

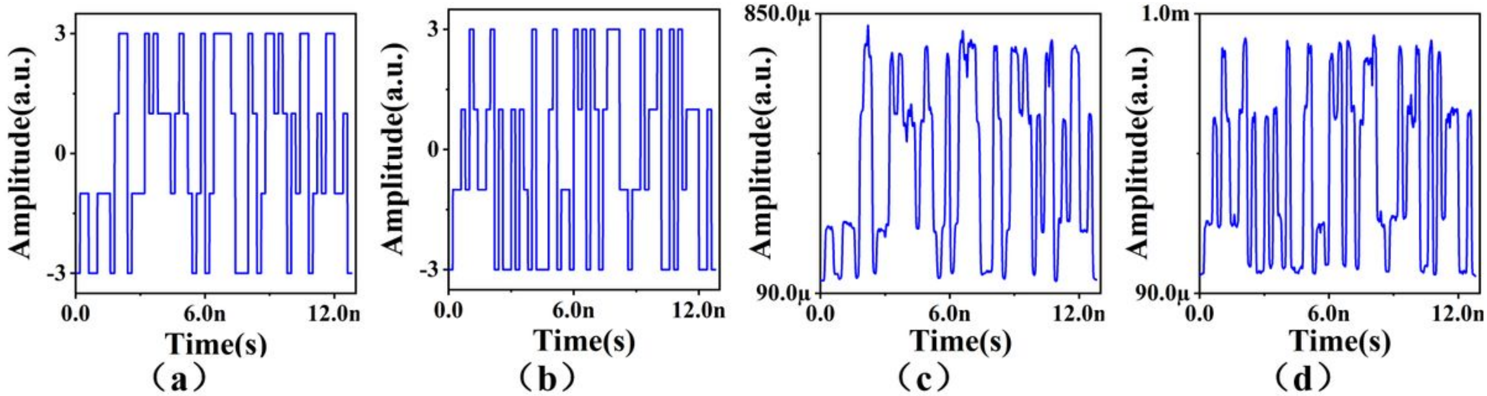

Figure 2

The time-domain waveforms before and after transmission

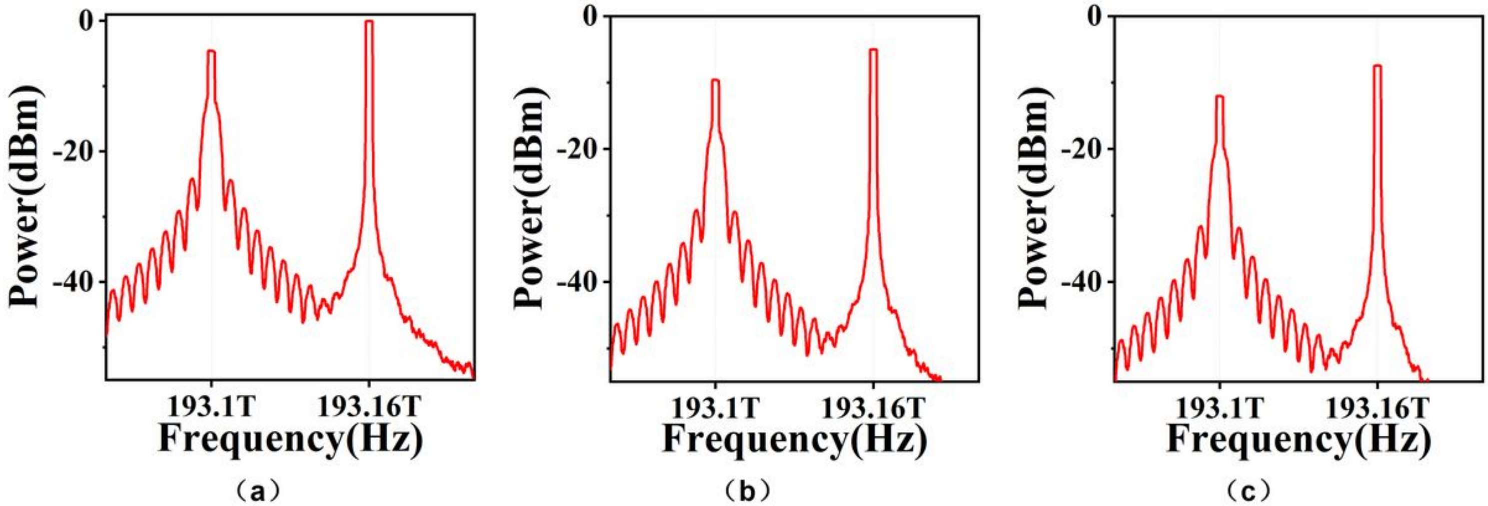

Figure 3

The optical spectra diagrams before transmission (a), after optical fiber transmission (b) and after FSO link transmission (c)

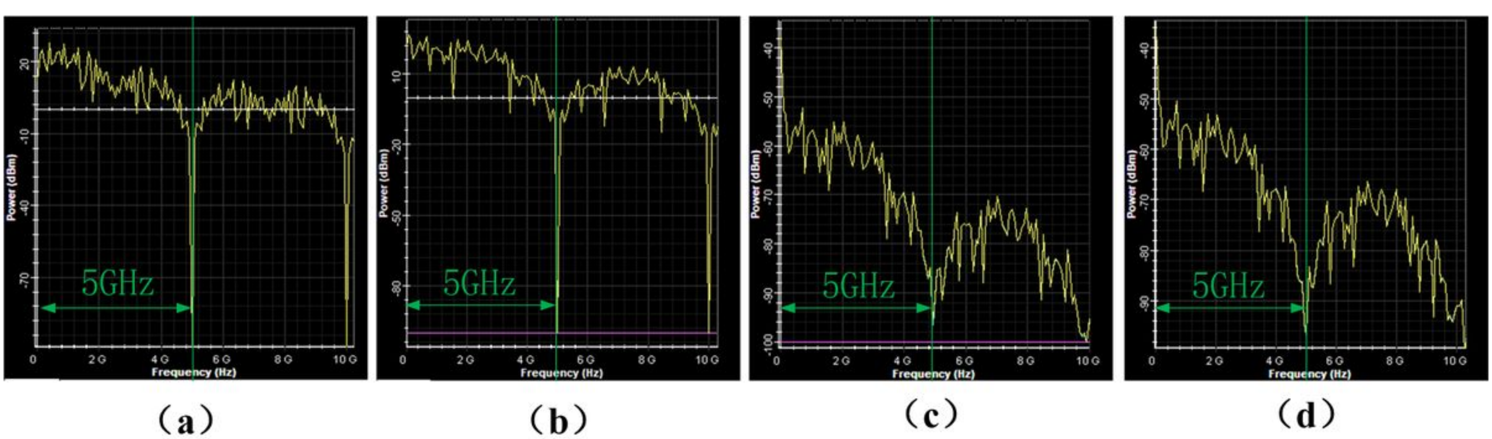

Figure 4

The demodulated electrical spectrums before and after transmission

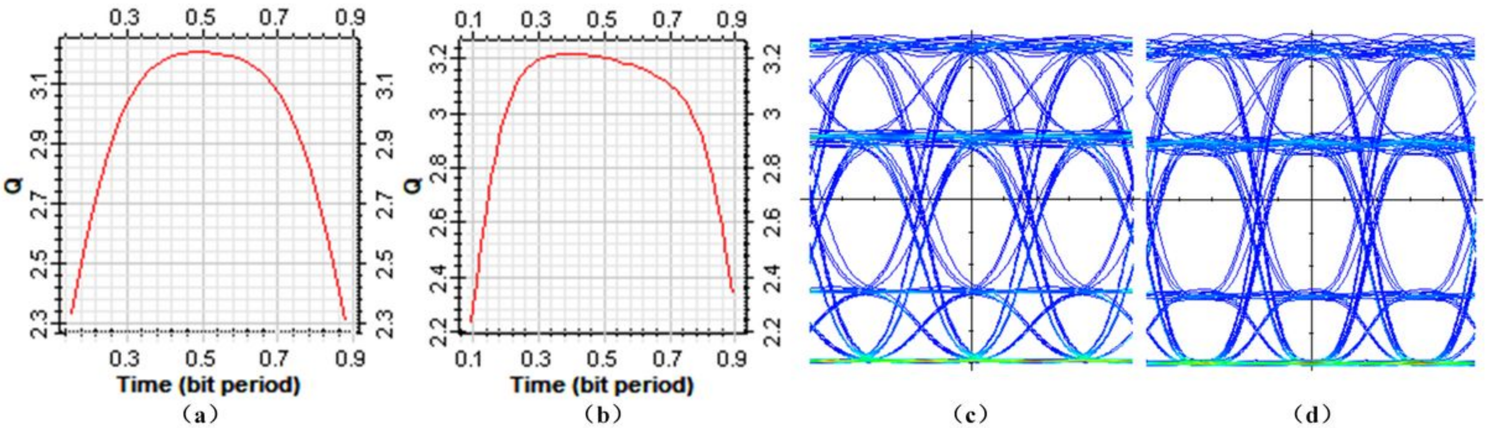

Figure 5

Q factors v/s bit period of PAM4 $signal_1$ (a) and PAM4 $signal_2$ (b). Eye diagrams of two depolarization multiplexing data signals, (c) is the received eye diagram of $data_1$, (d) is the received eye diagram of $data_2$

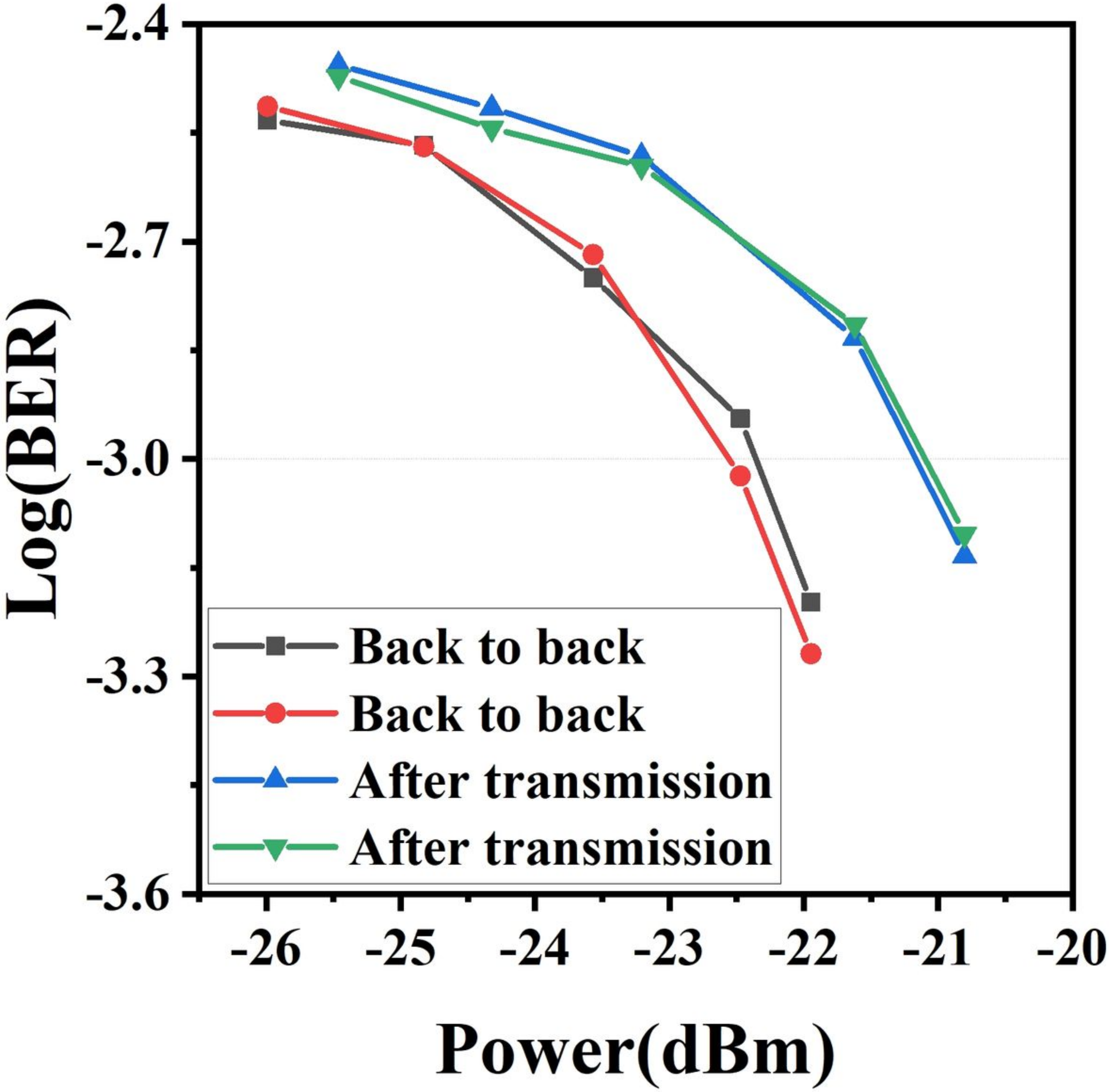

Figure 6

Received power versus BER after detecting signals.